Heliyon 6 (2020) e04216

Contents lists available at ScienceDirect

Heliyon

journal homepage: www.cell.com/heliyon

Research article

Genomic effects of a nanostructured alumina insecticide in human peripheral blood lymphocytes in vitro

Juan Vilchez-Aruani [a], Fernando D. Cuello-Carrión [b], Susana R. Valdez [c,d,1], Silvina B. Nadin [a,e,*,1]

[a] Laboratorio de Biología Tumoral, Instituto de Medicina y Biología Experimental de Cuyo (IMBECU), Consejo Nacional de Investigaciones Científicas y Técnicas (CONICET), Centro Científico Tecnológico (CCT) Mendoza, Argentina
[b] Laboratorio de Oncología, IMBECU, CONICET, CCT Mendoza, Argentina
[c] Laboratorio de Reproducción y Lactancia, IMBECU, CONICET, CCT Mendoza, Argentina
[d] Universidad Nacional de Cuyo, Facultad de Ciencias Exactas y Naturales, Mendoza, Argentina
[e] Universidad Nacional de Cuyo, Mendoza, Argentina

ARTICLE INFO

Keywords:
Molecular biology
Ecology
Nanomaterials
Pesticide
Biological sciences
Toxicology
Nanostructured alumina
Human peripheral blood lymphocytes
Cytotoxicity
Genotoxicity
Comet assay
Micronuclei

ABSTRACT

Nanotechnology is providing new tools for precision agriculture, such as agrochemical agents and innovative delivery mechanisms to improve cropping efficiency. Powder nanoinsecticides, such as experimental nanostructured alumina (NSA), show great potential for sustainable agriculture as an alternative to conventional synthetic pesticides because their mechanism of insecticide action is based on physical rather than on biochemical phenomena. However, even in highly non-reactive and hardly soluble substances such as alumina, reduced particle size may lead to an increased toxicity of the material. In order to determine whether NSA induces DNA and chromosomal damage, its toxicity was assessed in human peripheral blood lymphocytes (PBL) and contrasted with commercial nanostructured alumina, natural insecticide powders and a conventional pesticide. PBL from healthy donors were exposed for 24 h to increasing concentrations (50, 100 and 200 μg/mL) of NSA particle agglomerates (<350 nm); positive and negative NSA-particles, respectively; bulk Al_2O_3 (4.5 μm) or Diatomaceous Earth (SiO_2, <4.5 μm). Alkaline comet assay and micronuclei (MNi) test were used to assess DNA damage and chromosomal breakage, respectively. Cell viability was tested with resazurin assay. Comet assay results revealed no significant increase in DNA damage by NSA compared to other natural substances. As expected, DNA breaks were significantly higher in cells exposed to an organophosphate [OPP] control ($P < 0.05$). No statistically significant differences were found in terms of cellular viability at 50 and 100 μg/mL of NSA but cell survival decreased at 200 μg/mL as well as in OPP group. Positively charged NSA particles significantly reduced cell viability and increased DNA migration and oxidative DNA damage (8-oxoG). NSA as well as the electrically charged NSA particles had no significant effect on MNi induction. Our results indicate that NSA particles are non-cytotoxic and non-genotoxic at the tested doses and do not cause obvious DNA damage in human PBL in vitro.

1. Introduction

The use of synthetic organic pesticides has contributed to improving food production in terms of both yield and quality. Public awareness about the adverse effects of these products has, however, increased in recent years, raising the demand for food safety as well as for strict regulations on pesticide residues [1, 2].

The disadvantages of conventional synthetic organic pesticides have attracted enormous attention, coupling a strong public opinion with legislative and executive actions by state and federal governments. Active ingredients in pesticides became one of the most stringently regulated groups following a regimen that is similar to that for the preclinical assessment for the safety of a prescription drug [3]. Concurrently, the search for new active principles as alternatives to conventional pesticides has become a priority [4].

Part of the research on new, less toxic and environmentally friendly pesticides focuses on natural products such as plant extracts, essential oils and nanoengineered insecticides. The latter have long been promoted as

* Corresponding author.
E-mail address: snadin@mendoza-conicet.gob.ar (S.B. Nadin).
[1] These authors contributed equally to this work.

https://doi.org/10.1016/j.heliyon.2020.e04216
Received 25 September 2019; Received in revised form 11 February 2020; Accepted 11 June 2020

prospective alternatives to conventional synthetic organic pesticides. Nanoengineered insecticides have raised great interest among the international research community, with a significant increase in the number of publications devoted to the subject [5, 6]. The agroindustry is also intensively researching a new generation of nanobased plant protection products focused on the development of pesticide formulation with slow releasing properties and enhanced solubility, permeability and stability [7]. For example, components of conventional products are reduced to nanosize, leading to the reduction of the active substance quantities and a more efficient targeting and dosage [8]. Another approach is to pack the active ingredients in nanocapsules, making them stable to sunlight or alkaline environments [9]. Nanomaterials may also provide solutions to challenges in the areas of insect pest control by using them directly as an active ingredient [5]. The discovery of nano-insecticides based on synthesized nanomaterials, such as nanostructured alumina [10] and silica nanoparticles [11], provided new alternatives to expand the spectrum of applications of inorganic powders, opening new frontiers for nanotechnology in pest management. For example, nanostructured alumina (NSA) has been shown to have good insecticidal activity jointly with some of the characteristics of an ideal insecticide, given that it is an inert powder (not reactive), cost-effective and reduces the probability of resistance evolution in insects [12].

The mechanism of action of NSA is based on physical phenomena rather than on biochemical mechanisms typical of conventional synthetic organic insecticides. Electrostatic loaded NSA particles attach to the insect's body surface due to triboelectric forces. Then, interfacial forces between the adsorbate wax molecules and the adsorbent NSA powder [6, 13] remove the insect cuticle's protective wax layer, leading to dehydration-induced death of the insect [14].

NSA belongs to the class of nanoceramics, which are widely used in industrial products. Nonetheless, the acute toxicity and genotoxic effects of nanoalumina are not well known, and research on their toxicity remains limited. Variables such as particle size, shape, surface area and surface charge may play a crucial role in the toxicity of NSA. Even a small modification of some of these variables can result in a more or less marked change of a biological effect linked to cytotoxicity and reactive oxygen species (ROS) generation [15, 16, 17]. Nevertheless, it is important to mention that isolated nanoparticles rarely occur during NSA synthesis by combustion. The NSA combustion synthesis method leads to aggregates of strongly fused primary particles. The weak interaction forces between aggregates, such as van der Waals interactions and physical adhesion, lead to the formation of micro-sized agglomerates [18].

The first step in nanotoxicological studies comprises the assessment of toxic effects on cellular viability and genomic stability. Genotoxicity screening involves studying modifications ranging from DNA damage to chromosome aberrations. Cellular models are more appropriate than animal models in terms of ethical considerations, handling and costs [19]. In this context, human peripheral blood lymphocytes (PBL) represent easily accessible cells that are widely and frequently used for biomonitoring nanoparticle genotoxicity [20]. As demonstrated by Stadler et al., NSA has a highly efficient insecticide potential, shown in Sitophilus oryzae (L.) and Rhyzopertha dominicata (F.). Its toxicological effects have not yet been evaluated in normal human cells [6, 10].

The aim of our work was to determine the cytotoxic and genotoxic effects of nanostructured alumina NSA on human PBL in vitro, in order to contribute to the toxicological information necessary to fulfilling the toxicology data and hazard requirements in humans. In addition, NSA was compared with bulk aluminium oxide due to their differences in granulometry. NSA effects on DNA damage and cell viability were also contrasted against other insecticides, such as Diatomaceous Earth (DE: a natural inorganic powder) and an organophosphate (OPP: azinphos-methyl, a synthetic organic insecticide) known to be highly toxic for mammals. The alkaline comet assay and the micronuclei (MNi) test were used to evaluate genotoxicity (DNA strand breaks and chromosomal breakage) and the resazurin assay, which measures mitochondrial activity in living cells, to test for cytotoxicity. The oxidized DNA base 8-oxoguanine (8-oxoG) was employed as marker of oxidative DNA damage.

2. Materials and methods

2.1. Test substance characterization

a. Nanostructured alumina (Al_2O_3) (test substance) [experimental insecticide powder]

Experimental nanostructured alumina (NSA) samples were kindly provided by Dr Stadler to test their cytotoxicity and genotoxicity. NSA was synthesized with the glycine-nitrate combustion synthesis technique using a redox mixture, with glycine as fuel and aluminum nitrate nonahydrate as oxidizer, as described by Toniolo et al. [21]. The obtained NSA was previously characterized as a homogeneous powder of high purity (≈98%) with uniform characteristics and specific physicochemical properties, platelet morphology and an amorphous grain [6, 22, 23]. During the combustion process, NSA particles (40–60 nm) aggregate in primary clusters, building electrically loaded amorphous micrometric agglomerates with a surface area of 14 m^2/g and a size ranging from 0.1 to only a few micrometers and a readily evident platelet morphology [24]. Particle size analysis revealed a bi-modal size distribution with large particle aggregates of 1.5 μm and smaller particles with a diameter of ≥200 nm [22]. Figure 1 shows a representative image from scanning electron microscopy of NSA particle-agglomerates (<350 nm) that have been used in the subsequent bioassays. In addition, negative and positive NSA particles (Neg NSA; Pos NSA) were kindly provided by Dr. T. Stadler (IMBECU, CCT CONICET-Mendoza, Argentina). Neg NSA and Pos NSA particles were separated from newly synthesized NSA using copper electrodes plugged to a 6 Amp Key Tech power supply, as published by Stadler et al. [6]. Briefly, Neg NSA and Pos NSA particles were selected by electrostatic filtration, and loaded particles attached to the electrodes through Coulomb forces. NSA particles affixed to the respective collecting electrodes, and NSA particles unstuck at once from electrodes after the power supply was switched off [6].

b. Nanoalumina (Al_2O_3) [standard reference substance for NSA] Commercial nanoalumina (Al_2O3) (Sigma Aldrich, CAS# 1344-28-1)
c. Aluminium oxide (reference substance for Al_2O_3 bulk material)

Aluminium oxide (CAS# 1344-28-1, Kramer Industries, Inc), grit # 1000 mesh (small grain bulk aluminium oxide powder - treated control), (Al_2O_3 1000G): 97.69% Al_2O_3, grain shape angular, crystallinity coarse

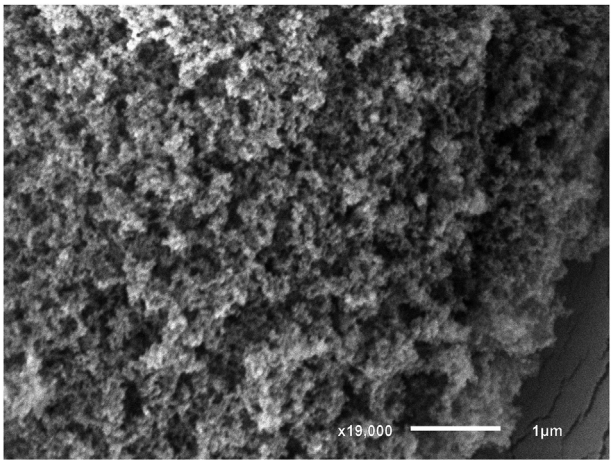

Figure 1. Scanning Electron Microscopy image of NSA particles agglomerates. Format JEOL/EO, Version 1.0. Instrument JSM-661; AccelVolt 10.; Signal SEI; Spot_Size 35. Vac Mode HV.

crystal, hardness 9 Mohs, specific gravity 3.8. Particle size = 4.5 μm (https://www.fepa-abrasives.com/abrasive-news/tag/standards).

d. Diatomaceous Earth (treated control; reference substance for natural inorganic insecticide powders)
   a. Commercial Diatomaceous Earth (DE) [DiatomiD®] obtained from fossilized sedimentary deposits of single-celled phytoplankton microalgae (diatoms) from San Juan-Argentina (CAS# 91053-39-3), which contains over 85% amorphous SiO_2. The median particle size is 10 μm, and particles range from 1 to 45 μm. Specific gravity is 0.22 [25].

b. Azinphos-methyl (treated control) (O,O-dimethyl-S-[(4-oxo-1,2,3-benzotriazin-3(4H)yl)methyl] phosphorodithioate); (synthetic organophosphate pesticide). Molecular Weight (MW): 317.3; Specific Gravity (SG): 1.44 at 20 °C; Water Solubility: 28 mg/L at 20 °C; Vapor pressure: 1.6×10^{-6} mmHg at 20 °C; Octanol/water partition coefficient: 360 at 20 °C. Azinphos-methyl is a broad-spectrum organophosphate insecticide (OPP), acaricide, and molluscacide. Azinphos-methyl and its oxygen analog produce their toxic reaction primarily through their inhibition of acetylcholinesterase. Azinphos-methyl was positive in selected in vitro genotoxicity assays, but in none of the in vivo assays. In addition, a study on the carcinogenicity of this OPP revealed no evidence of any carcinogenic effect in rats [26].

2.2. Isolation of lymphocytes and experimental procedures

For peripheral blood lymphocyte (PBL) isolation, 20 mL of venous blood were obtained by venipuncture from five clinically healthy donors (in two repetitions). Lymphocytes were separated from whole blood using Histopaque 1077 (Sigma Aldrich, St. Louis, MO, USA) and then cultured at 37 °C in RPMI 1640 medium supplemented with 10% fetal bovine serum, 5 μg/mL phytohemagglutinin, 2 mM L-glutamine, 100 U/mL penicillin and 100 μg/mL streptomycin. After 48 h incubation, PBLs were exposed for 24 h to: a) experimental NSA (Al_2O_3); b) 1000G; c) diatomaceous earth (DE); d) commercial NSA; e) negative (Neg) or f) positive (Pos) particles of experimental NSA. After exposure, cells were collected, fixed in 10% formalin buffer or cryopreserved at –80 °C for further comparative cytotoxicity and genotoxicity studies [27].

2.3. Cell viability

The viability of cells was evaluated using resazurin sodium salt (Sigma). Resazurin is a cell permeable redox indicator that can be used to monitor cell viability in the short-term [28]. The oxidized form of resazurin (blue) is reduced by cellular mitochondrial metabolism into resofurin, its reduced form (pink). The quantity of resofurin produced is proportional to the number of viable cells [29]. Cells were exposed during 24 h to increasing concentrations of experimental NSA and DE or Al_2O_3 1000G (50, 100 and 200 μg/mL). In another experiment, cells were exposed to 100, 200 and 400 μg/mL of experimental NSA and a reference commercial NSA during 24 h. After treatments, control and treated PBL (5×10^4 cells/well) were transferred to a 96-well microplate containing 180 μL RPMI 1640 medium and 20 μL of 700 μM oxidized resazurin stock solution (final concentration 70 μM). The cells were incubated at 37 °C in a humidified 5% CO_2 atmosphere. Four hours later, and after shaking, oxidized resazurin and resofurin were analyzed using a microplate reader (MULTISKAN EX; Thermo Scientific, Lafayette, CO, USA) at 570 nm and 620 nm [30, 31]. Test compounds and vehicle controls were included in the assay. As positive controls, 6 μg/mL doxorubicin (Filaxis Laboratory, Buenos Aires, Argentina) and 200 μg/mL OPP were used [27, 32]. The percentage of viability was determined by normalization of the 570/620 absorbance ratio to the untreated control cells. Each treatment was performed in triplicate.

2.4. Alkaline comet assay

One of the most commonly used methods to assess genotoxic damage is the single cell-gel electrophoresis assay (comet assay). It was first introduced to measure DNA strand breaks and has been extensively used to measure DNA damage at the individual cell level in various research areas [33]. The alkaline version of comet assay performed at pH > 12 allows the detection of Single-Strand Breaks (SSBs), Double-Strand Breaks (DSBs) and alkaline-labile sites in DNA [34]. For this, frozen PBLs were thawed in a thermostatic bath at 37 °C, washed in PBS and resuspended in cold PBS at a final concentration of 1×10^6 cells/mL. Cell viability tested with Trypan blue exclusion test was >95% in the control group. To prevent additional DNA damage, the assay was done in the dark and at 4 °C. Alkaline comet assay was performed as published elsewhere [27]. After electrophoresis, the agarose gels containing the cells were placed on microscope slides and silver stained as previously reported [35]. All samples were evaluated under the 20X objective, in duplicate and under double blindness using a Nikon Eclipse E200 microscope (Nikon, Japan), counting 40 cells/slide (i.e., 80 cells per specific treatment). A visual score based on the extent of DNA migration was used [36]. In addition, an average of DNA migration was calculated as [(% of cells with score 1)x1 + (% of cells with score 2)x2 + (% of cells with score 3)x3 + (% of cells with score 4)x4 + (% of cells with score 5)x5/100] [27]. As positive control, we used cells treated with 6×10^{-1} μg/mL of hydrogen peroxide for 1 h. The assay was done in duplicate.

2.5. Cytokinesis-block micronuclei cytome assay

Micronuclei (MNi) are chromatin-containing structures in the cytoplasm without any detectable link to the cell nucleus. They are biomarkers of chromosome breakage and/or whole chromosome loss. MNi are scored specifically in once divided binucleated cells. The procedure was done according to the protocol published by Fenech [37]. Briefly, human PBLs were incubated in RPMI 1640 medium and stimulated with 5 μg/mL phytohemagglutinin. Forty-four hours after culture initiation, cytochalasin B (Cyt-B) from a stock solution of 60 μg/mL was added to a final concentration of 4.5 μg/mL, together with the compounds to test. At 24 h after addition of Cyt-B, cells were harvested for slide preparation and scoring according to the procedure given by Fenech [37]. Slides were fixed for 5 min in absolute ethanol:acetic acid solution (3:1) and stained with 5% Giemsa. Samples were evaluated in duplicate under 100X objective using a Nikon Eclipse E200 microscope. All slides were reviewed and scored separately by two observers. DNA damage was scored in 200 binucleated (BN) cells and included: a) micronuclei (MNi), chromosome breakage and/or whole chromosome loss marker; b) nucleoplasmic bridges (NPBs), a biomarker of DNA misrepair and/or telomere end-fusions; and c) nuclear buds (NBUDs), a biomarker of elimination of amplified DNA and/or DNA repair complexes. Cytostatic effects were measured by calculating the proportion of mono-, bi- and multinucleated cells and cytotoxicity was assessed using necrotic and/or apoptotic cell ratios [37]. Doxorubicin (Filaxis laboratory, Argentina), an anticancer drug known to induce DNA fragmentation, was used at 10 μg/mL as positive control.

2.6. Immunocytochemistry

The presence of 8-oxoguanine (8-oxoG), a major product of oxidative DNA damage, was determined by immunocytochemistry [27]. After experimental treatments, PBLs were fixed in 10% buffered formalin at room temperature and smeared over precoated slides (3-aminopropyltriethoxysilane). For cell permeabilization, the slides were immersed 5 min in Triton X-100 0.5% in phosphate-buffered saline (PBS, pH 7.4) at 4 °C. Antigen unmasking was carried out in 0.01 M citrate buffer (pH 6.0) at 100 °C for 25 min after blocking endogen peroxidase

with 0.1% sodium azide. Samples were incubated with anti-8-oxoG mouse monoclonal antibody (Abcam, Cat# ab64548) at 1:200 dilution in humidity chambers overnight at 4 °C. A biotin-conjugated anti-mouse IgG (Vectastain ABC HRP kit, Vector Laboratories, USA) was used as second antibody according to the manufacturer's instructions. Diaminobenzidine (0.5 mg/ml)/hydrogen peroxide (0.01%) was used as chromogen substrate (ImmPACT DAB, Vector Laboratories). Slides were lightly counterstained with 0.5% methyl green and observed using an E-200 Nikon Eclipse microscope. The immunostaining was evaluated according to the percentage of positive cells (cytoplasmic or nuclear staining) by counting 200 cells per sample under double blindness. A negative control was included in each assay. Doxorubicin (Filaxis), anticancer drug well characterized by massive accumulation of reactive oxygen species (ROS) as central mechanism of toxicity, was used as positive control at 6 μg/mL.

2.7. Ethical statement

This study was approved by the Ethics Committee of the Medical School, National University of Cuyo, Mendoza, Argentina, in accordance with the Code of Ethics of the World Medical Association Declaration of Helsinki. Written informed consents were obtained from subjects included in the study.

2.8. Statistical analysis

Treatments were compared with Kruskal-Wallis signed rank nonparametric test with Dunn post-hoc test with a confidence interval of 95%. Statistical analyses were performed using GraphPad Prism Software version 6.01 (San Diego, CA, USA). P-values <0.05 were considered statistically significant.

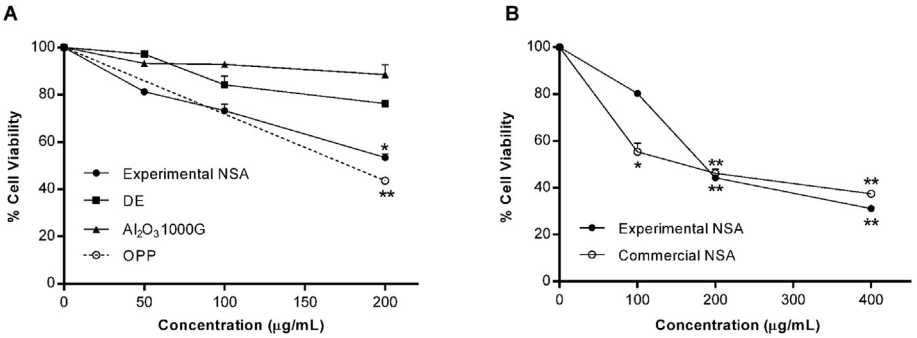

Figure 2. Viability curves of peripheral blood lymphocytes (PBL) from healthy subjects exposed to compounds for 24 h. A) Cytotoxic effect of experimental nanostructured alumina (NSA), diatomaceous earth or SiO_2 (DE) and Al_2O_3 1000G at increasing concentrations (50, 100 and 200 μg/mL). Treatment with the organophosphate azinphos-methyl (OPP) was used as positive control. B) Viability of PBL exposed to high concentrations of experimental and commercial NSA (100, 200 and 400 μg/mL). Experiments were performed twice and in triplicate. Viability is displayed as mean ± SEM. *P < 0.05. **P < 0.01.

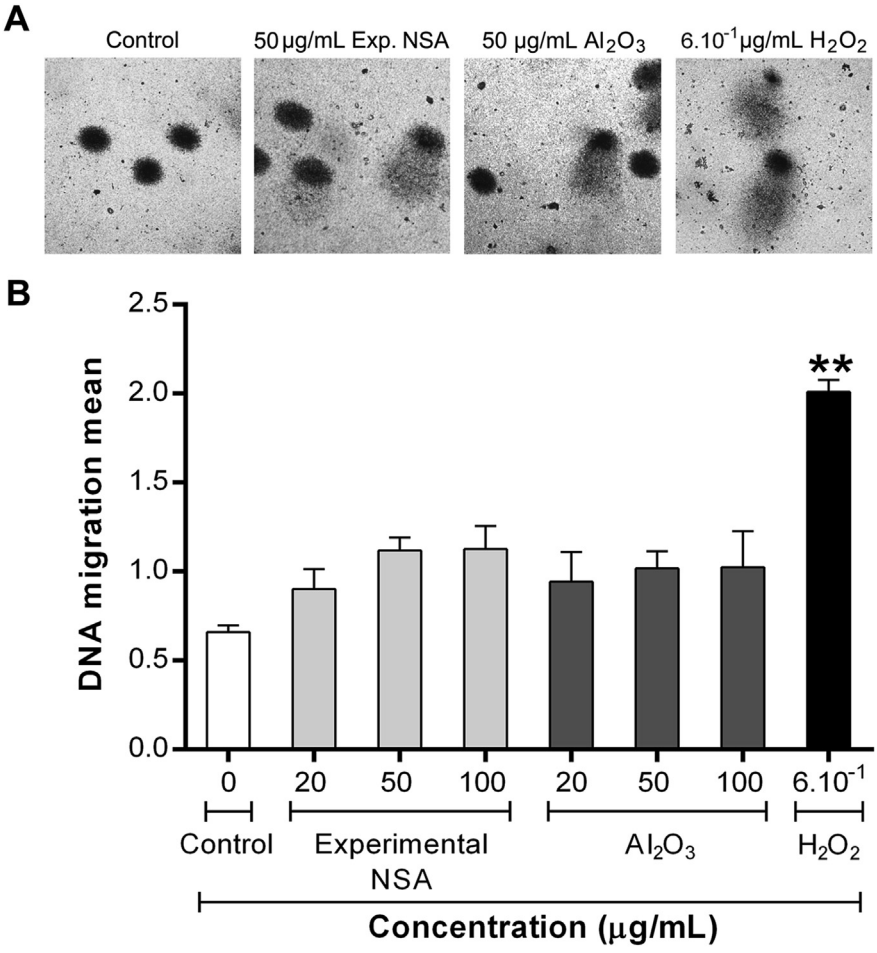

Figure 3. Comet assay mean DNA migration of human PBL exposed to experimental NSA and Al_2O_3 1000G at increasing concentrations for 24 h. A) Representative images of comets at basal conditions (Control) and after treatment with 50 μg/mL of experimental NSA and Al_2O_3 1000G. Images were taken under light microscope with a 40X objective. B) Quantitative representation of mean DNA migration at concentrations of 20, 50 and 100 μg/mL (mean ± SEM). No statistically significant changes were found between compounds. Hydrogen peroxide at 6.10^{-1} μg/mL was used as positive DNA migration control. **P < 0.01.

3. Results

3.1. Effects of experimental NSA on PBL viability. Comparisons with natural inorganic Al_2O_3 bulk material and insecticide powder compounds

Cell viability was assessed after 24 h exposure of PBL to increasing concentrations (50, 100 and 200 μg/mL) of experimental NSA and other inorganic non-nanostructured materials such as DE or Al_2O_3 1000G (4.5 μm particle size). There were no significant differences in cell viability between untreated control cells and PBL treated with the natural compounds (DE or Al_2O_3) (Figure 2 A). However, viability significantly decreased in cells treated with experimental NSA at a concentration of 200 μg/mL ($P < 0.05$). As expected, cells exposed to the positive control OPP (200 μg/mL) displayed a significantly lower viability than untreated control cells ($P < 0.01$; Figure 2 A).

Experimental NSA effects on cell viability were also contrasted against a reference commercial NSA. The percentage of viable cells significantly decreased equally (more than 40%) after 24 h treatment with both NSA particles at increasing concentrations (100, 200 or 400 μg/mL; Figure 2 B).

3.2. Effect of alumina nanoparticles and Al_2O_3 bulk material on DNA

To determine the effects of experimental NSA and Al_2O_3 1000G (Al_2O_3) on DNA migration, PBL were exposed for 24 h to increasing concentrations (20, 50 and 100 μg/mL) of the tested compounds (Figure 3 A). Alkaline comet assay revealed no statistically significant differences between the effect of both chemical substances. DNA damage induced by experimental NSA and Al_2O_3 1000G followed a similar behavior, without statistically significant differences compared to untreated control (Figure 3 B).

Mean DNA migration was measured after exposure to experimental NSA, Al_2O_3 1000G or DE at a concentration of 200 μg/mL. The compounds induced a non-significant, mild increase of the mean DNA migration values (Figure 4 A and B). In contrast, a significantly higher mean DNA migration ($P < 0.05$) was observed after treatment with the OPP at a concentration of 200 μg/mL.

DNA damage was evaluated in parallel experiments after exposure to increasing concentrations of the experimental and a commercial NSA (100, 200 and 400 μg/mL). PBL were exposed for 24 h and doxorubicin (6 μg/mL) was used as positive control. None of these substances affected the mean DNA migration at elevated concentrations. As expected, only doxorubicin significantly increased DNA migration ($P < 0.01$) compared to the untreated control group (Figure 5 A and B).

3.3. Analysis of oxidative DNA damage

The effect of experimental and commercial NSA on human PBL was tested using 8-oxoguanine (8-oxoG) as an oxidative DNA damage marker. Because no differences were observed between experimental NSA and DE or bulk Al_2O_3 in terms of cell viability and DNA damage, we only explored the oxidative effects of the experimental NSA, as mentioned above. Cells were treated with 200 μg/mL of each compound for 24 h. A group of cells treated with 6 μg/mL doxorubicin was used as positive control. Immunocytochemistry revealed that both experimental and commercial NSA did not increase levels of 8-oxoG compared to untreated control cells. By contrast, doxorubicin significantly increased ($P < 0.05$) the percentage of 8-oxoG positive cells (Figure 6).

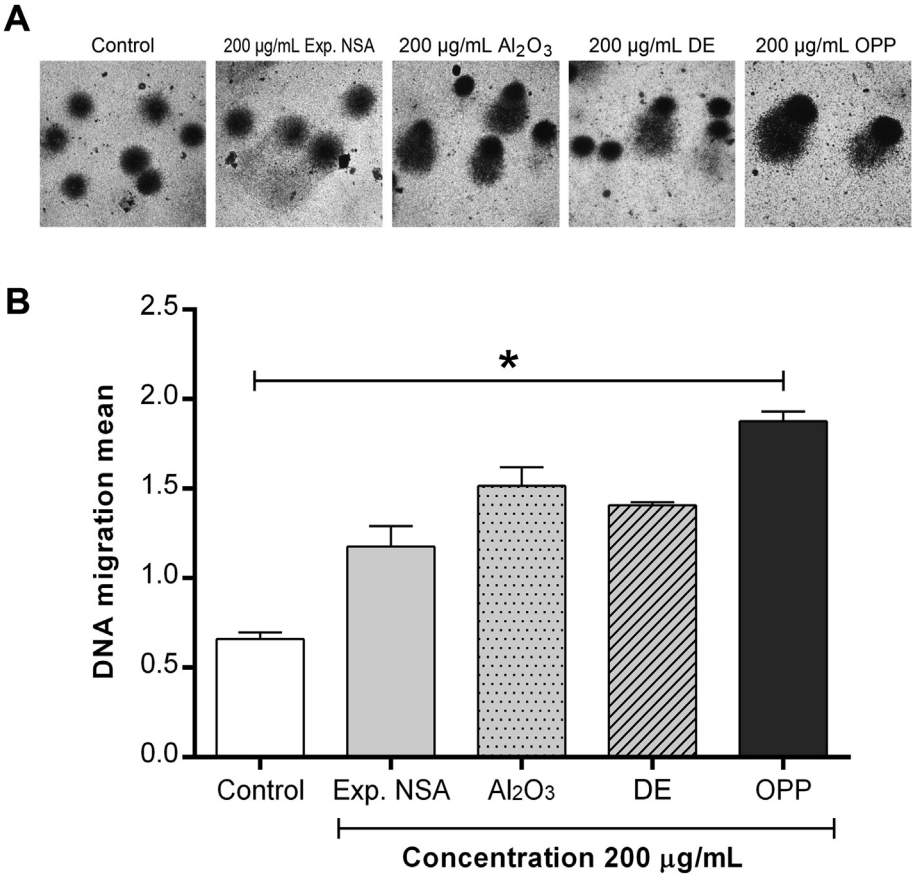

Figure 4. Mean of DNA migration in human PBL exposed to 200 μg/mL of experimental NSA and other natural compounds for 24 h. A) Comet assay images of PBL at basal conditions (Control) and after treatment with 200 μg/mL of experimental NSA, Al_2O_3 1000G, DE and OPP. Images were taken from an optical microscope with a 40X objective. B) Histograms of mean DNA migration after exposure to experimental NSA, Al_2O_3 1000G, DE and OPP showing mean ± SEM. The tested compounds did not significantly increase the mean DNA migration. Hydrogen peroxide at 6.10^{-1} μg/mL was used as positive DNA migration control. **$P < 0.01$.

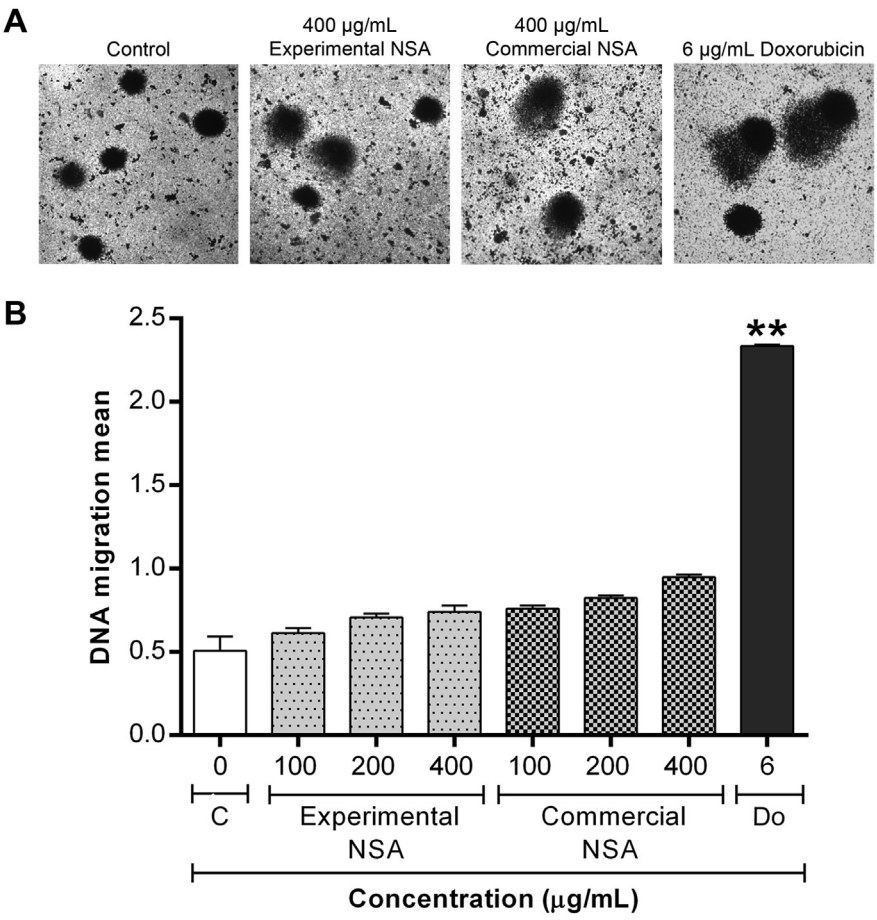

Figure 5. Effects of experimental and commercial NSA on mean DNA migration of PBL. A) Comet assay pictures at basal conditions and after treatment with 400 µg/mL of experimental and commercial NSA. Images were taken under light microscope with a 40X objective. B) Histograms of mean DNA migration ±SEM after exposure to 100, 200 and 400 µg/mL of experimental and commercial NSA. The levels of DNA damage compared to the untreated control (C) were not significant. Doxorubicin (Do) at 6 µg/mL was used as positive control. **P < 0.01.

3.4. Nanoparticle surface charge effects on cell viability, DNA fragmentation and oxidative DNA damage

Human PBL were treated during 24 h with 100, 200 or 400 µg/mL of positively charged NSA particles (Pos NSA) or negatively charged NSA particles (Neg NSA). The percentage of viable cells decreased approximately 20% after exposure to Neg NSA particles, but it remained close to 80% at all tested concentrations (Figure 7). Surprisingly, treatment with Pos NSA particles reduced the number of viable cells by 50–55%, but no statistically significant differences were seen between Pos NSA and Neg NSA at any concentration.

The effect of nanoparticle charge on DNA damage was also measured at different concentrations (100, 200 and 400 µg/mL). Comet assay

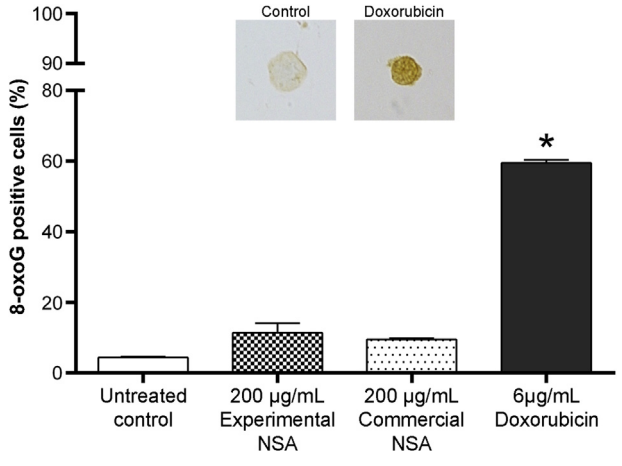

Figure 6. Oxidative DNA damage evaluated by 8-oxoG immunostaining in PBL treated with 200 µg/mL of experimental and commercial NSA. No statistically significant changes were found in comparison with untreated cells (Control). Cells treated with 6 µg/mL doxorubicin for 24 h were used as positive control for oxidative DNA damage. The inserts show images of negative and positive 8-oxoG immunostaining in untreated and doxorubicin-treated PBL, respectively. Bars represent mean ± SEM. *P < 0.05.

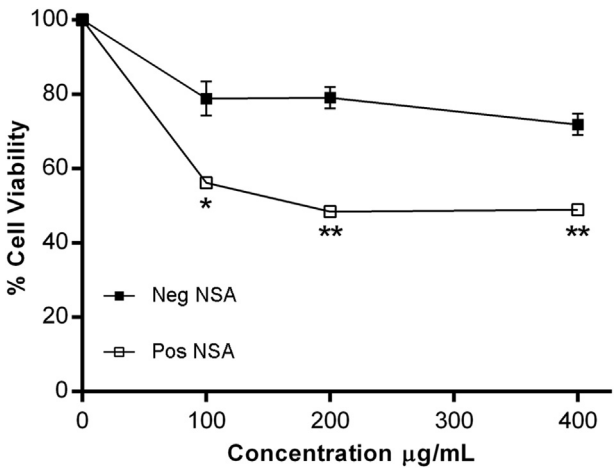

Figure 7. Effect of surface charge on cell viability. Positively charged NSA particles were more cytotoxic than negatively charged NSA particles at concentrations of 100, 200 and 400 µg/mL. Each point of the curve represents the mean ± SEM. *P < 0.05. **P < 0.01. Positively charged NSA particles: Pos NSA. Negatively charged NSA particles: Neg NSA.

results showed that treatment with both Pos NSA and Neg NSA significantly increased mean DNA migration at all concentrations tested. However, no statistically significant differences in mean DNA migration were found between Pos NSA and Neg NSA (Figure 8 A and B).

In order to establish whether the DNA damage observed with comet assay was a result of oxidative stress, 8-oxoG was measured in PBL after treatment with 200 μg/mL of Pos NSA or Neg NSA. The percentage of 8-oxoG positive cells increased to about 25% after treatment with Pos NSA particles ($P < 0.05$; Figure 9).

3.5. Alumina nanostructured NSA effect on chromosome aberrations

The cytokinesis-block micronuclei cytome assay measures the damage induced to the chromosomes and mitotic apparatus. Genotoxic effects of 200 μg/mL experimental NSA, Pos NSA and Neg NSA were evaluated in PBL. Commercial NSA was used as reference product. Doxorubicin was used as positive control at 10 μg/mL for 24 h. As shown in Table 1, experimental, commercial or charged NSA did not induce MNi at the tested concentrations. An increased frequency of MNi was found only in the positive control group exposed to doxorubicin.

4. Discussion

Nanotechnology has revolutionized different areas through the development of innovative technologies in different areas. In the agricultural field, the use of chemical pesticide formulations is being revised because of their serious implications to human health and their negative environmental effects. Here, nanopesticides emerge as suitable alternatives with a range of benefits [38]. Alumina-based nanoparticles have been proposed as an alternative to prevent stored grains pests. Previous results have shown that nanostructured alumina have an insecticidal activity similar to that of commercially available insecticidal powders [10, 22]. In the present work we have explored the cytotoxic and genotoxic properties of nanostructured alumina (NSA) in human peripheral blood lymphocytes.

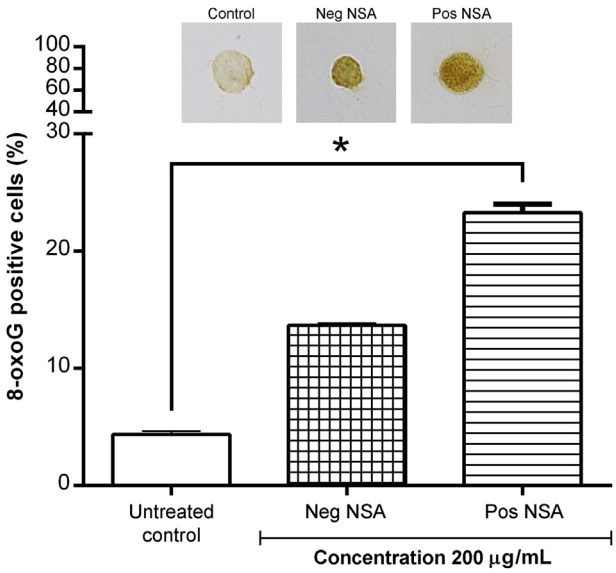

Figure 9. Oxidative damage in lymphocytes exposed to charged NSA particles. Positively charged NSA particles increased the percentage of 8-oxoG positive cells. The immunostaining images in the inserts show representative PBL with an increased intensity reaction for 8-oxoG induced by positively charged NSA particles exposure. Bars represent mean ± SEM. *P < 0.05. Positively charged NSA particles: Pos NSA. Negatively charged NSA particles: Neg NSA.

A cytotoxic compound induces a short-term loss of cell viability. Cell viability was tested with bulk Al_2O_3, nanostructure alumina (NSA) and DE. These synthetical and natural substances did not cause changes in the percentage of viable cells, but the viability significantly decreased (near

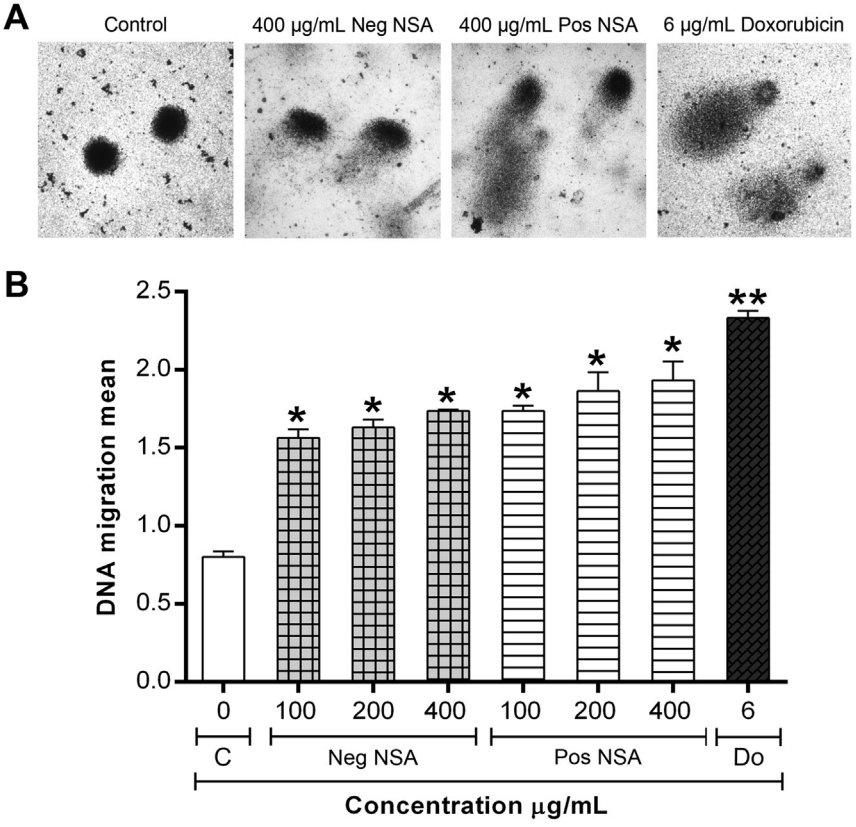

Figure 8. DNA damage in PBL exposed to negatively and positively charged NSA particles. A) Representative silver stained comets in untreated control cells and in PBL exposed to experimental NSA separated by charge at a concentration of 400 μg/mL. Note that the DNA damage induced by positively charged NSA particles was higher than that induced by negatively charged NSA. Images were obtained from a light microscope using a 40X objective. B) The DNA damage induced by charged particles was greater than control (C). Cells treated with 6 μg/mL of doxorubicin (Do) for 24 h were used as positive control. Bars represent mean ± SEM. *P < 0.05. **P < 0.01. Positively charged NSA particles: Pos NSA. Negatively charged NSA particles: Neg NSA.

Table 1. Effects of nanostructured alumina on chromosomal aberrations.

	% MonoN cells	% BN cells	% MultiN cells	% apoptotic cells	% necrotic cells	% BN cells with MNi
Untreated control	51.5 ± 0.866	48.0 ± 0.577	0.5 ± 0.288	0.00	0.00	0.00
10 μg/mL Doxorubicin	38.5 ± 4.619	44.0 ± 0.866	10.0 ± 1.732	5.0 ± 0.012*	2.5 ± 0.866	22.5 ± 2.598**
200 μg/mL Commercial NSA	47.5 ± 3.175	50.5 ± 0.288	2.0 ± 1.555	0.00	0.00	0.00
200 μg/mL Experimental NSA	57.0 ± 3.464	41.0 ± 3.464	2.0 ± 0.577	0.00	0.00	0.00
200 μg/mL Neg NSA	49.5 ± 1.732	41.0 ± 0.288	8.0 ± 2.309	1.0 ± 0.577	0.5 ± 0.288	0.00
200 μg/mL Pos NSA	57.0 ± 2.887	38.0 ± 2.021	3.5 ± 0.287	0.5 ± 0.288	1.0 ± 0.577	0.5 ± 0.288

MonoN: mononucleated cells. **BN:** binucleated cells. **MultiN:** multinucleated cells, cells with three or more nuclei. **MNi:** micronuclei.
Neg NSA: negatively charged NSA. **Pos NSA:** positively charged NSA.
This data is presented as mean ± SEM. *P < 0.05. **P < 0.01.

50%) at the highest final experimental NSA concentration (200 μg/mL or 2 mM). Hence, it is probable that cytotoxicity had a dose-dependent behavior and was related to particle size, from bulk to nano. Sliwinska and collaborators have shown that metal oxide nanoparticles (ZnO-NPs and Al_2O_3-NP) at ≥0.5 mM slightly reduced the viability of lymphocytes [39]. In the case of SiO_2 NP, it has been demonstrated that they reduce replication activity to 60% after 24 h of exposure [40]. In another study, Wagner and colleagues estimated the cytotoxic activity of aluminium oxide NP (mean size 40 nm) after 24 h of exposure in cell lines from rat alveolar macrophages. No changes in cell viability were observed at concentrations as high as 250 μg Al_2O_3/mL [41]. Moreover, aluminum oxide NP with grain size averages of 50–80 nm, and agglomerates of 230–550 nm, have shown to cause a low (<10%) cytotoxic effect in murine and human normal skin fibroblasts exposed for 24 h to concentrations ranging from 10 to 400 μg/mL [42]. In A549 human lung epithelium cell lines, exposure to various nanoparticles showed that aluminum oxide NP had a lower cytotoxic effect than nanometric titanium dioxide and carbon nanotubes [43]. It has also been demonstrated that Al_2O_3 (16.7 nm) NP were not cytotoxic at different concentrations (1, 10 and 100 μg/mL) in human peripheral blood lymphocytes [44]. All of these reports support our observations that NSA cytotoxicity is related to particle size. In this sense, Wei et al. found that smaller Al_2O_3 NP (10 nm) had a higher cytotoxicity than those of 50 nm [45]. Finally, DE did not induce significant changes in cellular viability. In accordance with our observations, another study has shown that DE from different regions does not constitute a single entity and that its toxic potential ranges from unreactive to cytotoxic depending on other minerals and impurities present in the crystal structure [46].

Different studies have shown that NP toxicity can depend not only on their size, but also on their surface area, chemistry, charge, structure and agglomeration, among other factors [47, 48]. Dong et al. have shown that cell toxicity of gamma nanoalumina (γ-NA) was low [49]. Furthermore, the loss of cell viability was dose-dependent at γ-NA concentrations below 200 μg/mL. The generation of ROS can, however, contribute to the cytotoxicity of alumina particles at high concentrations without inducing cell death [49].

We also investigated the effects of NSA on DNA damage using the alkaline comet assay. Our results indicate that experimental NSA, non-nanostructured Al_2O_3 (dose range 20–100 μg/mL) and DE cause similar levels of DNA damage, which are also similar to control cells. As expected, OPP positive control increases DNA damage compared to untreated control. In human cell cultures at high concentrations, azinphosmethyl caused significant cell damage and cell viability decreased at 100 and 1000 μg/mL, by ROS generation mechanisms [50]. On the other hand, many studies testing aluminum oxide NP effects on DNA did not observe severe DNA damage induction. For instance, Demir and collaborators demonstrated by comet assay that aluminum oxide NP (16.7 nm) does not induce DNA damage at concentrations of 1–100 μg/mL in human peripheral blood lymphocytes and cultured embryonic kidney cells [44]. No cytotoxic or genotoxic effects were found in monkey kidney cell lines and prokaryotic cells exposed to aluminum oxide NP [51].

In contrast to these findings, a few studies have shown the potential of alumina nanoparticles to induce DNA damage in human cells. Exposure of human peripheral blood lymphocytes to concentrations >0.5 mM Al_2O_3 NP caused a concentration-dependent increase in DNA single-strand breaks and oxidative DNA damage but did not trigger apoptosis [39]. Alarifi and collaborators reported a significant increase in DNA damage in human hepatocarcinoma cells (HepG2) exposed for 24 and 48 h to Al_2O_3 NP (mean particle size <30–60 nm) at concentrations of 50, 150 and 450 μg/mL [52]. Alumina NP of 13 and 50 nm have also been shown to induce DNA damage at concentrations of 15, 30 and 60 μg/mL in Chinese hamster lung fibroblast cells [53]. Nanomaterials may be able to enter directly into the nucleus through diffusion across the nuclear membrane and transport through nuclear pore complexes, where they can interact directly with the DNA molecule [54]. Nevertheless, our data indicate that even at elevated concentrations, experimental NSA does not disrupt the DNA structure. Future studies of our research group will focus on the uptake of nanostructured NSA across the plasma membrane and their effects on cell membrane charge using other cellular models.

On the other hand, some studies have reported that NP induce ROS generation and that the involved mechanisms are NP type dependent. In most cases, oxidative stress caused by metal-based NP (such as Cu and Fe) is conducted via Fenton-type reactions through an increase in membrane lipid peroxidation and ROS production [55, 56]. It is well documented that oxidative stress represents a key factor in nanotoxicity, affecting a variety of cellular components such as DNA. DNA damage induced by NP has been attributed to the generation of hydroxyl free radical (HO•) that interacts with DNA and causes guanine oxidation, forming 8-hydroxyl-2‘-deoxyguanosine (8-oxoG) [57, 58]. However, we found similar levels of 8-oxoG in untreated control lymphocytes and those exposed to experimental NSA. In contrast, 8-oxoG levels increased after treatment with positively charged NSA particles (Pos NSA), which was also associated with increased DNA fragmentation and reduced cell viability. According to our observations, oxidative-DNA damage caused by Pos NSA may be attributed to an indirect effect of NSA on DNA through its ability to generate ROS. It has been proposed that oxidative stress induced by alumina NP is mainly due to ROS mediated mechanism [59]. Aluminum oxide NP (particle size 30–60 nm) have shown cytotoxic and genotoxic effects in HepG2 cells through ROS-triggered mitochondrial apoptotic pathway of cell death [52]. In accordance with our results, Shao et al. reported that positively charged polymeric nanoparticles with higher charges offered higher interaction forces with cells and induced significant cytotoxicity in mouse L929 fibroblasts

[60]. Other studies have also demonstrated that positively charged polystyrene NP were more cytotoxic than negatively charged NP on HeLa and NIH/3T3 cells [61]. The elevated toxicity of positively charged NP can be explained by their ability to interact with negatively charged cell membrane glycoproteins. We observed that Pos NSA and Neg NSA induced similar levels of DNA damage measured by comet assay, but Neg NSA did not cause a significant increase in 8-oxoG levels. Xu and colleagues showed that the charge of NP can be changed through modifications of their surface. Consequently, polymer NP that were negatively charged in a neutral medium changed to a positive charge in an acid medium at pH 5–6 [62]. We therefore hypothesize that Neg NSA particles could be changing their surface charge into positive as an effect of the cellular metabolism, which in turn may alter the pH of the medium. Further studies will be needed to corroborate these associations and ROS production mechanisms involved in the cytotoxicity of charged NSA particles.

The final step of this study was to detect chromosomal aberrations after NSA exposure. A previous study with Al_2O_3 NP (<30 nm and 40 nm) revealed no increase in DNA fragmentation in peripheral rat lymphocytes after oral exposure [63]. A more recent report indicated that Al_2O_3 NP did not cause DNA damage in human peripheral lymphocytes or chromosomic aberrations at concentrations of 10, 25, 50, 75 and 100 μg/mL for 24 h [64]. Moreover, nanoalumina particles at concentrations ranging from 1-10 mg/T-75 flask weakly increased micronucleus frequencies, chromosomal loss, gain mutations and polyploidy, but no sister chromatid exchanges were found to take place [65, 66]. In agreement with other authors, our findings indicate that experimental or charged NSA particles do not enhance the frequency of MNi, even at higher concentrations. Hence, NSA is not genotoxic for human PBL at the concentrations tested.

5. Conclusion

Nanostructured alumina (NSA) is a nano-engineered material with previously characterized insecticide properties. In this study we investigated for the first time the in vitro cytotoxicity and genotoxicity of NSA in human samples, thus contributing to the knowledge of the toxicological properties of this compound to evaluate the safety of its application in agriculture. Our results demonstrated that experimental NSA only showed a very low cytotoxicity in human PBL at the highest tested concentrations. We found that NSA did not affect the genome, except in the case of charged NSA particles that augmented DNA migration. Furthermore, positively charged NSA particles increased oxidative DNA damage through 8-oxoG formation in DNA. The latter may be a result of an oxidative stress mechanism only induced by positively charged nanostructured particles, as experimental NSA may not interact directly with DNA or alter genome stability. Also, experimental NSA did not cause chromosomal aberrations; hence, it was not mutagenic or genotoxic. Future studies should focus on determining the toxicological effects of NSA on oxidative stress in vitro and in vivo based on the magnitude of electric charges. In addition, toxicity research studies should determine the pharmacokinetic mechanisms involved after oral or inhalation exposure to NSA. Our results highlight that the tested compound could be safe for human health or the environment when used as a natural insecticide alternative in comparison with other organic synthetic products.

Declarations

Author contribution statement

J. Vilchez-Aruani and F. Cuello-Carrión: Performed the experiments; Analyzed and interpreted the data.

S. Valdez and S. Nadin: Conceived and designed the experiments; Performed the experiments; Analyzed and interpreted the data; Contributed reagents, materials, analysis tools or data; Wrote the paper.

Funding statement

This work was supported by CONICET (National Reasearch Council of Argentina), grant number PIP 2014–2016 GI (11220130100382CO).

Competing interest statement

The authors declare no conflict of interest.

Additional information

No additional information is available for this paper.

Acknowledgements

We want to thank Dr. Mariella Superina for helping us with grammar checking and manuscript editing and Dr. Teodoro Stadler for providing test material and related technical information, as well as for his kind contribution to the supervision of the experimental procedures.

References

[1] C.A. Damalas, Understanding benefits and risks of pesticide use, Sci. Res. Essays 4 (2009) 945–949.
[2] F.P. Carvalho, Pesticides, environment, and food safety, Food Energy Secur. 6 (2017) 48–60.
[3] P. Steinberg, High-throughput Screening Methods in Toxicity Testing, first ed., John Wiley & Sons Inc., New Jersey, 2013.
[4] V. Pelaez, G. Mizukawa, Diversification strategies in the pesticide industry: from seeds to biopesticides, Ciência Rural. 47 (2017).
[5] M. Kah, T. Hofmann, Nanopesticide research: current trends and future priorities, Environ. Int. 63 (2014) 224–235.
[6] T. Stadler, M. Buteler, S.R. Valdez, J.G. Gitto, Particulate Nanoinsecticides: a new concept in insect pest management. Insecticides - Agriculture and Toxicology, Ghousia Begum, IntechOpen, 2018.
[7] Werdin González, J.O., Gutiérrez, M.M., Ferrero, A.A., Fernández Band, B., 2014. Essential oils nanoformulations for stored-product pest control - characterization and biological properties. Chemosphere 100, 130-138. .
[8] M. Nuruzzaman, M.M. Rahman, Y. Liu, R. Naidu, Nanoencapsulation, nano-guard for pesticides: a new window for safe application, J. Agric. Food Chem. 64 (2016) 1447–1483.
[9] M.A. Robles-García, F. Rodríguez-Félix, E. Márquez-Ríos, J.A. Aguilar, A. Barrera-Rodríguez, J. Aguilar, S. Ruiz-Cruz, C.L. Del-Toro-Sánchez, Applications of nanotechnology in the agriculture, food, and pharmaceuticals, J. Nanosci. Nanotechnol. 16 (2016) 8188–8207.
[10] T. Stadler, M. Buteler, D.K. Weaver, Novel use of nanostructured alumina as an insecticide, Pest Manag. Sci. 66 (2010a) 577–579.
[11] N. Debnath, S. Das, D. Seth, R. Chandra, S.Ch. Bhattacharya, A. Goswami, Entomotoxic effect of silica nanoparticles against *Sitophilus oryzae* (L.), J. Pest. Sci. 84 (2011) 99–105.
[12] T. Stadler, M. Buteler, D.K. Weaver, Nanoinsecticidas: nuevas perspectivas para el control de plagas, Rev. Soc. Entomol. Argent. 69 (2010b) 149–156.
[13] P.C. Hiementz, Principle of Colloid and Surface Chemistry, second ed., Dekker Press, New York, 1986.
[14] T. Stadler, G.P. López García, J.G. Gitto, M. Buteler, Nanostructured alumina: biocidal properties and mechanism of action of a novel insecticide powder, Bull. Insectol. 70 (2017) 17–25.
[15] S. Bhattacharjee, L.H. de Haan, N.M. Evers, X. Jiang, A.T. Marcelis, H. Zuilhof, I.M. Rietjens, G.M. Alink, Role of surface charge and oxidative stress in cytotoxicity of organic monolayer-coated silicon nanoparticles towards macrophage NR8383 cells, Part. Fibre Toxicol. 7 (2010) 25.
[16] I. Pujalté, I. Passagne, B. Brouillaud, M. Tréguer, E. Durand, C. Ohayon-Courtès, B. L'Azou, Cytotoxicity and oxidative stress induced by different metallic nanoparticles on human kidney cells, Part. Fibre Toxicol. 8 (2011) 10.
[17] E. Maser, M. Schulz, U.G. Sauer, M. Wiemann, L. Ma-Hock, W. Wohlleben, A. Hartwig, R. Landsiedel, In vitro and in vivo genotoxicity investigations of differently sized amorphous SiO_2 nanomaterials, Mutat. Res. Genet. Toxicol. Environ. Mutagen 794 (2015) 57–74.
[18] E.V. Karaseva, A.A. Onischuk, V.V. Karasev, C.J. Tsai, High-speed video observations of the alumina nanoparticle formation during combustion of Al microparticles, in: European Aerosol Conference, Salzburg, Abstract T14A038, 2007. http://www.gaef.de/eac2007/eac2007abstracts/T14Abstractpdf/T14A038.pdf.
[19] C.T. Ng, J.J. Li, B.H. Bay, L.Y. Yung, Current studies into the genotoxic effects of nanomaterials, J. Nucleic Acids 2010 (2010) 947859.
[20] H. Norppa, Cytogenetic biomarkers, IARC Sci. Publ. 157 (2004) 179–205.
[21] C. Toniolo, From coded to non-coded alpha-amino acids: a journey in oligopeptide stereochemistry, J. Pept. Sci. 11 (2005) 250–253.

[22] T. Stadler, M. Buteler, D.K. Weaver, S. Sofie, Comparative toxicity of nanostructured alumina and a commercial inert dust for *Sitophilus oryzae* (L.) and *Rhyzopertha dominica* (F.) at varying ambient humidity levels, J. Stored Prod. Res. 48 (2012) 81–90.

[23] M. Buteler, S.W. Sofie, D.K. Weaver, D. Driscoll, J. Muretta, T. Stadler, Development of nanoalumina dust as insecticide against *Sitophilus oryzae* and *Rhyzopertha dominica*, Int. J. Pest Manag. 61 (2015) 80–89.

[24] V.V. Karasev, A.A. Onischuk, O.G. Glotov, A.M. Baklanov, A.G. Maryasov, V.E. Zarko, V.N. Panilova, A.I. Levykin, K.K. Sabelfeld, Formation of charged aggregates of Al_2O_3 nanoparticles by combustion of aluminum droplets in air, Combust. Flame 138 (2004) 40–54.

[25] M.L. Bilbao, M.O. Mañá, F. Murúa, Evaluation of the insecticidal effect of diatomaceous earth on *Triatoma infestans* (Hemiptera, Reduviidae), Rev. Peru. Med. Exp. Salud Pública 24 (2007) 179–181.

[26] WHO, Food and Agriculture Organization of the United Nations, FAO Panel of Experts on Pesticide Residues in Food and the Environment & WHO Core Assessment Group on Pesticide Residues, Pesticide Residues in Food: 2007, Toxicological Evaluations, Sponsored Jointly by FAO and WHO, with the Support of the International Programme on Chemical Safety, Joint Meeting of the FAO Panel of Experts on Pesticide Residues in Food and the Environment and the WHO Core Assessment Group, World Health Organization, Geneva, Switzerland, 2009, pp. 18–27. September 2007, http://www.who.int/iris/handle/10665/44064.

[27] S.B. Nadin, L.M. Vargas-Roig, G. Drago, J. Ibarra, D.R. Ciocca, DNA damage and repair in peripheral blood lymphocytes from healthy individuals and cancer patients: a pilot study on the implications in the clinical response to chemotherapy, Canc. Lett. 239 (2006) 84–97.

[28] M.D. Fellows, M.R. O'Donovan, Cytotoxicity in cultured mammalian cells is a function of the method used to estimate it, Mutagenesis 22 (2007) 275–280.

[29] S.A. Ahmed, R.M. Gogal Jr., J.E. Walsh, A new rapid and simple non-radioactive assay to monitor and determine the proliferation of lymphocytes: an alternative to [^{3}H]thymidine incorporation assay, J. Immunol. Methods 170 (1994) 211–224.

[30] J. O'Brien, I. Wilson, T. Orton, F. Pognan, Investigation of the Alamar Blue (resazurin) fluorescent dye for the assessment of mammalian cell cytotoxicity, Eur. J. Biochem. 267 (17) (2000) 5421–5426.

[31] T.L. Riss, R.A. Moravec, A.L. Niles, et al., Cell viability assays, in: G.S. Sittampalam, N.P. Coussens, K. Brimacombe, et al. (Eds.), Assay Guidance Manual [Internet], Eli Lilly & Company and the National Center for Advancing Translational Sciences, Bethesda (MD), 2013, 2004. Available from: https://www.ncbi.nlm.nih.gov/books/NBK144065/.

[32] U. Undeğer, N. Başaran, Effects of pesticides on human peripheral lymphocytes in vitro: induction of DNA damage, Arch. Toxicol. 79 (3) (2005) 169–176.

[33] O. Ostling, K.J. Johanson, Microelectrophoretic study of radiation-induced DNA damages in individual mammalian cells, Biochem. Biophys. Res. Commun. 123 (1984) 291–298.

[34] X. Pu, Z. Wang, J.E. Klaunig, Alkaline comet assay for assessing DNA damage in individual cells, Curr. Protoc. Toxicol. 65 (2015) 1–11.

[35] S.B. Nadin, L.M. Vargas-Roig, D.R. Ciocca, A silver staining method for single-cell gel assay, J. Histochem. Cytochem. 49 (2001) 1183–1186.

[36] D. Anderson, T.W. Yu, B.J. Phillips, P. Schmezer, The effect of various antioxidants and other modifying agents on oxygen-radical-generated DNA damage in human lymphocytes in the COMET assay, Mutat. Res. 307 (1994) 261–271.

[37] M. Fenech, Cytokinesis-block micronucleus cytome assay, Nat. Protoc. 2 (2007) 1084–10104.

[38] E.A. Worrall, A. Hamid, K.T. Mody, N. Mitter, H.R. Pappu, Nanotechnology for plant disease management, Agronomy 8 (2018) 285.

[39] A. Sliwinska, D. Kwiatkowski, P. Czarny, J. Milczarek, M. Toma, A. Korycinska, J. Szemraj, T. Sliwinski, Genotoxicity and cytotoxicity of ZnO and Al_2O_3 nanoparticles, Toxicol. Mech. Methods 25 (2015) 176–183.

[40] M. Chen, A. von Mikecz, Formation of nucleoplasmic protein aggregates impairs nuclear function in response to SiO_2 nanoparticles, Exp. Cell Res. 305 (2005) 51–62.

[41] A.J. Wagner, C.A. Bleckmann, R.C. Murdock, A.M. Schrand, J.J. Schlager, S.M. Hussain, Cellular interaction of different forms of aluminum nanoparticles in rat alveolar macrophages, J. Phys. Chem. B 111 (2007) 7353–7359.

[42] E. Radziun, J. Dudkiewicz Wilczyńska, I. Książek, K. Nowak, E.L. Anuszewska, A. Kunicki, A. Olszyna, T. Ząbkowski, Assessment of the cytotoxicity of aluminium oxide nanoparticles on selected mammalian cells, Toxicol. Vitro 25 (2011) 1694–1700.

[43] A. Simon-Deckers, B. Gouget, M. Mayne-L'hermite, N. Herlin-Boime, C. Reynaud, M. Carrière, In vitro investigation of oxide nanoparticle and carbon nanotube toxicity and intracellular accumulation in A549 human pneumocytes, Toxicology 253 (2008) 137–146.

[44] E. Demir, D. Burgucu, F. Turna, S. Aksakal, B. Kaya, Determination of TiO_2, ZrO_2, and Al_2O_3 nanoparticles on genotoxic responses in human peripheral blood lymphocytes and cultured embryonic kidney cells, J. Toxicol. Environ. Health A. 76 (2013) 990–1002.

[45] Z. Wei, L. Chen, D.M. Thompson, L.D. Montoya, Effect of particle size on in vitro cytotoxicity of titania and alumina nanoparticles, J. Exp. Nanosci. 9 (2014) 625–638.

[46] C. Nattrass, C.J. Horwell, D.E. Damby, A. Kermanizadeh, D.M. Brown, V. Stone, The global variability of diatomaceous earth toxicity: a physicochemical and in vitro investigation, J. Occup. Med. Toxicol. 10 (2015) 23.

[47] A. Albanese, P.S. Tang, W.C. Chan, The effect of nanoparticle size, shape, and surface chemistry on biological systems, Annu. Rev. Biomed. Eng. 14 (2012) 1–16.

[48] D. Battal, A. Çelik, G. Güler, A. Aktaş, S. Yildirimcan, K. Ocakoglu, Ü. Çömelekoğlu, SiO_2 Nanoparticule-induced size-dependent genotoxicity - an in vitro study using sister chromatid exchange, micronucleus and comet assay, Drug Chem. Toxicol. 38 (2015) 196–204.

[49] E. Dong, Y. Wang, S.T. Yang, Y. Yuan, H. Nie, Y. Chang, L. Wang, Y. Liu, H. Wang, Toxicity of nano gamma alumina to neural stem cells, J. Nanosci. Nanotechnol. 11 (2011) 7848–7856.

[50] J. Cortés-Eslava, S. Gómez-Arroyo, F. Arenas-Huertero, S. Flores-Maya, M.E. Díaz-Hernández, M.E. Calderón-Segura, R. Valencia-Quintana, J.J. Espinosa-Aguirre, R. Villalobos-Pietrini, The role of plant metabolism in the mutagenic and cytotoxic effects of four organophosphorus insecticides in Salmonella typhimurium and in human cell lines, Chemosphere 92 (2013) 1117–1125.

[51] R. Sadiq, Q.M. Khan, A. Mobeen, A.J. Hashmat, In vitro toxicological assessment of iron oxide, aluminium oxide and copper nanoparticles in prokaryotic and eukaryotic cell types, Drug Chem. Toxicol. 38 (2015) 152–161.

[52] S. Alarifi, D. Ali, S. Alkahtani, Nanoalumina induces apoptosis by impairing antioxidant enzyme systems in human hepatocarcinoma cells, Int. J. Nanomed. 10 (2015) 3751–3760.

[53] Q. Zhang, H. Wang, C. Ge, J. Duncan, K. He, S.O. Adeosun, H. Xi, H. Peng, Q. Niu, Alumina at 50 and 13 nm nanoparticle sizes have potential genotoxicity, J. Appl. Toxicol. 37 (2017) 1053–1064.

[54] A. Panariti, G. Miserocchi, I. Rivolta, The effect of nanoparticle uptake on cellular behavior: disrupting or enabling functions? Nanotechnol. Sci. Appl. 5 (2012) 87–100.

[55] Y.W. Huang, C.H. Wu, R.S. Aronstam, Toxicity of transition metal oxide nanoparticles: recent insights from in vitro studies, Materials (Basel) 3 (2010) 4842–4859.

[56] Y. Wang, W.G. Aker, H.M. Hwang, C.G. Yedjou, H. Yu, P.B. Tchounwou, A study of the mechanism of in vitro cytotoxicity of metal oxide nanoparticles using catfish primary hepatocytes and human HepG2 cells, Sci. Total Environ. 409 (2011) 4753–4762.

[57] T. Xia, M. Kovochich, J. Brant, M. Hotze, J. Sempf, T. Oberley, C. Sioutas, J.I. Yeh, M.R. Wiesner, A.E. Nel, Comparison of the abilities of ambient and manufactured nanoparticles to induce cellular toxicity according to an oxidative stress paradigm, Nano Lett. 6 (2006) 1794–1807.

[58] A. Abdal Dayem, M.K. Hossain, S.B. Lee, K. Kim, S.K. Saha, G.M. Yang, H.Y. Choi, S.G. Cho, The role of reactive oxygen species (ROS) in the biological activities of metallic nanoparticles, Int. J. Mol. Sci. 18 (2017) E120.

[59] E. Oesterling, N. Chopra, V. Gavalas, X. Arzuaga, E.J. Lim, R. Sultana, D.A. Butterfield, L. Bachas, B. Hennig, Alumina nanoparticles induce expression of endothelial cell adhesion molecules, Toxicol. Lett. 178 (2008) 160–166.

[60] X.R. Shao, X.Q. Wei, X. Song, L.Y. Hao, X.X. Cai, Z.R. Zhang, Q. Peng, Y.F. Lin, Independent effect of polymeric nanoparticle zeta potential/surface charge, on their cytotoxicity and affinity to cells, Cell Prolif 48 (2015) 465–474.

[61] Y. Liu, W. Li, F. Lao, Y. Liu, L. Wang, R. Bai, Y. Zhao, C. Chen, Intracellular dynamics of cationic and anionic polystyrene nanoparticles without direct interaction with mitotic spindle and chromosomes, Biomaterials 32 (2011) 8291–8303.

[62] P. Xu, E.A. Van Kirk, Y. Zhan, W.J. Murdoch, M. Radosz, Y. Shen, Targeted charge-reversal nanoparticles for nuclear drug delivery, Angew Chem. Int. Ed. Engl. 46 (26) (2007) 4999–5002.

[63] A. Balasubramanyam, N. Sailaja, M. Mahboob, M.F. Rahman, S.M. Hussain, P. Grover, In vivo genotoxicity assessment of aluminium oxide nanomaterials in rat peripheral blood cells using the comet assay and micronucleus test, Mutagenesis 24 (2009) 245–251.

[64] S. Rajiv, J. Jerobin, V. Saranya, M. Nainawat, A. Sharma, P. Makwana, C. Gayathri, L. Bharath, M. Singh, M. Kumar, A. Mukherjee, N. Chandrasekaran, Comparative cytotoxicity and genotoxicity of cobalt (II, III) oxide, iron (III) oxide, silicon dioxide, and aluminum oxide nanoparticles on human lymphocytes in vitro, Hum. Exp. Toxicol. 35 (2016) 170–183.

[65] A.L. Di Virgilio, M. Reigosa, P.M. Arnal, M. Fernández Lorenzo de Mele, Comparative study of the cytotoxic and genotoxic effects of titanium oxide and aluminium oxide nanoparticles in Chinese hamster ovary (CHO-K1) cells, J. Hazard Mater. 177 (2010) 711–718.

[66] A. Tsaousi, E. Jones, C.P. Case, The in vitro genotoxicity of orthopaedic ceramic (Al_2O_3) and metal (CoCr alloy) particles, Mutat. Res. 697 (2010) 1–9.